Progress in Oceanography 242 (2026) 103662

Contents lists available at ScienceDirect

Progress in Oceanography

journal homepage: www.elsevier.com/locate/pocean

Interannual variability and depth-dependence in pathways of Iceland–Scotland Overflow Waters exiting the Iceland Basin

Ali Johnson Exley [a,*], Amy Bower [a], Xiaobiao Xu [b], Sijia Zou [c], Anna Pinckney [a], Heather Furey [a]

[a] Woods Hole Oceanographic Institution, Woods Hole, MA, USA
[b] Center for Ocean-Atmospheric Prediction Studies, Florida State University, Tallahassee, FL, USA
[c] State Key Laboratory of Marine Environmental Science and College of Ocean and Earth Sciences, Xiamen University, Xiamen, China

ARTICLE INFO

Dataset link: https://www.hycom.org/, https://doi.org/10.26025/1912/24388, https://doi.org/10.26025/1912/24388, https://www.ncei.noaa.gov/archive/accession/0270533

Keywords:
Iceland Scotland Overflow Water
North Atlantic Current
Subpolar gyre dynamics

ABSTRACT

Iceland–Scotland Overflow Water (ISOW), a dense water mass formed in the Nordic Seas, spills into the Iceland Basin through the Iceland-Faroe Ridge and Faroe Shetland Channel before propagating southwestward along the eastern flank of the Reykjanes Ridge as a deep boundary current, contributing to the lower limb of the Atlantic Meridional Overturning Circulation. Recent work has demonstrated that pathways of ISOW out of the Iceland Basin are complex and variability has not been explored on interannual and longer timescales. In this study, we use the basin-scale, eddy-rich (1/12°), 40-year Atlantic Hybrid Coordinate Ocean Model (HYCOM) simulation to investigate the variability in ISOW export pathways. Simulated Lagrangian particles are released within the ISOW layer (σ_0 > 27.80 kg m^{-3}) at two locations along the eastern flank of the Reykjanes Ridge and classified according to their export pathway: over the Reykjanes Ridge, through the Charlie Gibbs Fracture Zone (CGFZ) or into the Western European Basin (WEB). We show that export over the Reykjanes Ridge exhibits variability on timescales from 2.5 years to decadal and is strongly correlated with mid-depth northward transport into the Iceland Basin forced by fluctuations in the North Atlantic Current (NAC), suggesting a link to large-scale gyre dynamics. Export through the CGFZ is characterized by variability of 2.5–5 years and is influenced by the meridional position of the eastward-flowing NAC within the CGFZ, which can block ISOW export and divert particles into the WEB. Export pathways are shown to exhibit a significant depth-dependence such that shallower layers are more strongly impacted by the surface circulation while deeper layers are more subject to topographic steering, results that are corroborated by utilizing observations from RAFOS floats deployed during the OSNAP campaign. Together, these findings illustrate the high-degree of variability in pathways of ISOW export and contributes to the growing body of evidence that challenges the notion of a single, dominant pathway out of the Iceland Basin.

1. Introduction

The Meridional Overturning Circulation (MOC) plays a fundamental role in Earth's climate system by redistributing heat and freshwater between the equator and poles and by sequestering carbon in the ocean interior. In the subpolar North Atlantic, the southward transport of dense North Atlantic Deep Water (NADW), is the primary component of the lower limb of the MOC. While significant attention has been given to the formation of these deep water masses, their downstream pathways and variability are equally critical for constraining rates of overturning on interannual and longer timescales (Devana and Johns, 2024). Investigating these pathways, and their drivers, is therefore essential for quantifying the strength and structure of the overturning, especially as the MOC is expected to respond to anthropogenic warming.

NADW is largely composed of Labrador Sea Water (LSW), formed by wintertime deep convection, and overflows from the Nordic Seas. Namely, Denmark Strait Overflow Water (DSOW) and Iceland–Scotland Overflow Water (ISOW). While pathways of DSOW demonstrate some mesoscale variability, the overflow largely spills over the Denmark Strait into the Irminger Sea and continues along eastern Greenland as a well-documented boundary current (Dickson and Brown, 1994; Yashayaev and Dickson, 2008). In contrast, pathways of ISOW out of the Iceland Basin are more complex and therefore less understood (Lozier et al., 2022). ISOW originates in the Nordic Seas where

* Corresponding author.
E-mail address: alexis.exley@whoi.edu (A.J. Exley).

https://doi.org/10.1016/j.pocean.2025.103662
Received 14 July 2025; Received in revised form 16 December 2025; Accepted 29 December 2025
Available online 30 December 2025

wintertime cooling and brine rejection during sea ice formation creates a dense water mass that spills over the Iceland-Faroe Ridge and Faroe-Shetland Channel (Hansen and Østerhus, 2000; Beaird et al., 2013). As it descends into the Iceland Basin, ISOW entrains warmer and saltier subpolar Mode Water (SPMW) and smaller volumes of ambient LSW. The resulting water mass is characteristically saltier (>34.94 psu) than other components of NADW and typically defined as water with potential density between 27.80 and 27.88 kg m^{-3} (Saunders, 1994; Hansen and Østerhus, 2000).

Historically, the majority of ISOW was thought to travel southwestward along the Reykjanes Ridge (Saunders, 1994, 1996), exiting the Iceland Basin via the Charlie Gibbs Fracture Zone, and continuing on into the Irminger Sea as a deep cyclonic boundary current (Swift, 1984). However, long-term Eulerian observations along the path of ISOW within the Iceland Basin have challenged this traditional theory. Collectively, overflow from the Faroe-Shetland Channel and Iceland-Faroe Ridge is estimated to be about 3 Sverdrups total (1 Sverdrup, Sv $\equiv 1 \times 10^6$ m^3 s^{-1}) (Hansen and Østerhus, 2007; Hansen et al., 2016). Downstream, transport increases to about 5 Sv near the Bight Fracture Zone (BFZ), suggesting significant entrainment and modification of ISOW along the eastern flank of the Reykjanes Ridge (Saunders, 1996; Kanzow and Zenk, 2014; Johns et al., 2021). Within the CGFZ however, multiple mooring arrays have measured a westward ISOW transport of around 2 Sv (Saunders, 1994; Bower and Furey, 2017). The substantial decrease in transport between the BFZ and CGFZ implies a significant portion of ISOW finds alternate export pathways out of the Iceland Basin.

Observations and modeling work has largely reconciled these transport differences by confirming the existence of multiple ISOW spreading pathways out of the Iceland Basin and, more broadly, within the subpolar North Atlantic (Fig. 1). Recent model results suggest submesoscale structures near the southernmost tip of the Iceland Shelf diverges ISOW into multiple pathways within the interior Iceland Basin (De Marez et al., 2024). Further downstream, Xu et al. (2010) uses an eddy-rich North Atlantic simulation to demonstrate that, in addition to westward flow through the CGFZ, a significant portion of upper layer ISOW is exported to the Irminger Sea through the BFZ and other gaps in the Reykjanes Ridge. Hydrography and deep float trajectories corroborate these model results (Kanzow and Zenk, 2014; Daniault et al., 2016; Petit et al., 2019, 2022) and, more recently, moored observations have been used to estimate a mean westward ISOW transport of 0.6 ± 0.3 Sv through the BFZ (Furey et al., 2024). In addition to pathways through gaps in the Reykjanes Ridge, Zou et al. (2017) uses simulated particles released within the eddy-rich FLAME model to suggest that a significant portion (~20%) of ISOW is also exported southward, into the Western European Basin (WEB), along the eastern flank of the Mid-Atlantic Ridge.

Deep RAFOS floats released during the Overturning in the Subpolar North Atlantic Program (OSNAP) have verified both Reykjanes Ridge and WEB export pathways and simultaneously challenged our understanding of the deep boundary current within the Irminger Sea (Zou et al., 2020; Lozier et al., 2022). Of the 61 floats released in the Iceland Basin and within the CGFZ, not a single float conclusively followed the boundary current through CGFZ and northward along the western flank of the Reykjanes Ridge. Alternatively, floats to successfully traverse through the CGFZ either traveled northwestward, taking a direct route to the Labrador Sea, or southward along the eastern flank of the Mid-Atlantic Ridge. Zou et al. (2020) suggested meanders associated with the North Atlantic Current (NAC) could be responsible for the relatively strong southward spreading observed within the RAFOS floats.

While these studies have reshaped our understanding of ISOW spreading pathways within the subpolar gyre, they highlight the need to better constrain the variability in these pathways and their drivers, as they influence the timing and structure of NADW export from the region. Several mooring arrays in the Iceland Basin, including the near decade-long OSNAP record, have explored this question from a

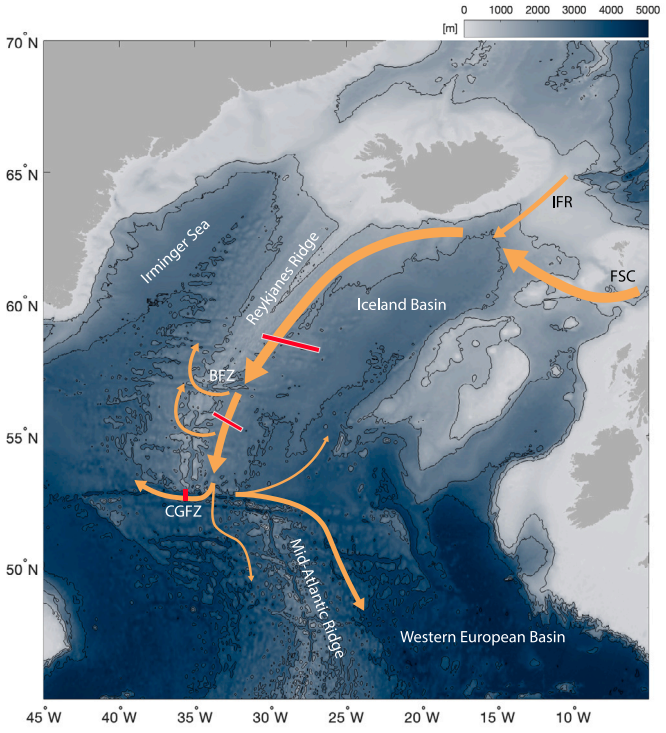

Fig. 1. A schematic of Iceland–Scotland Overflow Water spreading pathways out of the Iceland Basin. Three solid red lines indicate the locations where RAFOS floats used in this study were released. Solid red lines outlined in white indicate the locations where simulated particles were released (co-located with float release locations east of the Reykjanes Ridge). Abbreviations are Charlie Gibbs Fracture Zone (CGFZ), the Bight Fracture Zone (BFZ), Iceland-Faroe Ridge (IFR) and Faroe-Shetland Channel (FSC).

Eulerian framework north of the BFZ (Saunders, 1996; Kanzow and Zenk, 2014; Johns et al., 2021; Devana and Johns, 2024). Transport estimates from these mooring arrays reveal significant variability on sub-seasonal timescales, with no singular dominant period. Kanzow and Zenk (2014) demonstrate that flow changes are linked to variations in hydrographic properties, suggesting that much of the ISOW variability upstream of the BFZ results from lateral water mass exchange during entrainment. They also attribute higher frequency current fluctuations to topographic Rossby waves propagating along the slope. Additionally, Johns et al. (2021) and De Marez et al. (2024) suggests deep reaching mesoscale eddies associated with the NAC drive variability in the offshore component of the ISOW plume.

Within the BFZ, a single mooring array has documented strong seasonal variability in ISOW transport through gaps in the Reykjanes Ridge, with peak transport occurring during the summer and fall months and weak transport, or even eastward reversals in the flow, occurring in the winter and spring (Furey et al., 2024). The numerical model outputs of Xu et al. (2018) also indicate that transport over the ridge is characterized by a strong seasonal cycle. The underlying drivers of this seasonal variability however remain unknown.

As the primary exit pathway of ISOW out of the Iceland Basin, a significant amount of work has focused on quantifying the strength and variability of ISOW through the CGFZ. Saunders (1994) identified strong variability in ISOW transport through the CGFZ over a large range in temporal scales. Eventually, this variability was linked to northward intrusions of the largely barotropic eastward-flowing NAC, which can temporarily block or deflect ISOW from successfully traveling through the CGFZ (Schott et al., 1999; Bower and von Appen, 2008; Bower and Furey, 2017; Xu et al., 2018). Deep Lagrangian floats within the ISOW layer have also revealed that the NAC can exert a

strong influence on ISOW pathways leaving the CGFZ (Zou et al., 2020) and locally enhances mixing between ISOW and surrounding water masses (Racapé et al., 2019).

Missing from our understanding, however, is a holistic view of how ISOW pathways out of the Iceland Basin interact over longer timescales and contribute to large-scale ISOW export and NADW formation. While individual pathways have been studied in isolation, we lack a clear picture of their interannual variability, associated drivers, and how these pathways are interconnected. Also missing, is an understanding of how these pathways change with depth. Significant progress has been made addressing transport variability across various ISOW pathways from the Iceland Basin, however much of this focus has been on bulk transport changes as ISOW is often treated as a single, uniform layer. However, ISOW spans a broad depth range (~1500–3000+ m), and its pathways out of the Iceland Basin, as well as its distribution throughout the subpolar North Atlantic, likely differ depending on depth. Furthermore, the circulation of ISOW within and beyond the Iceland Basin occurs within the broader context of the cyclonic subpolar gyre. This large-scale system, driven by wind and buoyancy forcing, governs the mean flow field and likely provides the dynamical backdrop for ISOW export and recirculation. Establishing how ISOW pathways are linked to variability in the subpolar gyre represents an important step toward a more complete understanding of deep circulation in the subpolar North Atlantic.

The aim of this study is to reconstruct ISOW spreading pathways and their variability within a Lagrangian framework. To accomplish this we employ output from the HYbrid Coordinate Ocean Model and seed simulated particles within the ISOW layers on the eastern flank of the Reykjanes Ridge. Simulated, 10-year particle trajectories are corroborated with a subset of isobaric RAFOS floats released during the OSNAP program that freely drifted around the subpolar North Atlantic for two years. The combination of particle trajectories and RAFOS floats extends our observational lifespan and provide a valuable Lagrangian framework that insures we capture continuous movement of ISOW through complex bathymetry and across multiple exit pathways from the Iceland Basin. These datasets, as well as our methodology, are described in Section 2. In Section 3, we document the interannual variability, its drivers, and interconnectedness of ISOW pathways out of the Iceland Basin. We then introduce a strong depth-dependency in Section 4, with a particular focus on particle export from the CGFZ. Findings are validated with observational data in Section 5 and we summarize and conclude in Section 6.

2. Data and methods

2.1. HYbrid Coordinate Ocean Model

Output from the basin-scale Atlantic simulation based on the HYbrid Coordinate Ocean Model (HYCOM) (Bleck, 2002; Chassignet et al., 2003) is used in this study to investigate pathways of ISOW within the subpolar North Atlantic. The vertical coordinate of HYCOM is isopycnic in the stratified ocean interior and dynamically transitioned to fixed pressure levels in the surface mixed layer. The simulation is restarted from a climatological spin-up (10 years) and is interannually forced over the period of 1978–2022 using a combination of atmospheric reanalysis products: the European Center for Medium Range Weather Forecasts reanalysis (ERA40) (Uppala et al., 2005) for 1978–2001, the Navy Operational Global Atmospheric Prediction System (NOGAPS) (Rosmond, 1992) for 2002–2012 and the Navy Global Environmental Model (NAVGEM) (Hogan et al., 2014) for 2013–2022, both from the US Navy's Fleet Numerical Meteorology and Oceanography Center. The simulation is a nature run without data assimilation.

The model domain covers the North and Equatorial Atlantic Ocean from 28°S to 80°N. No inflow/outflow are prescribed at northern and southern boundaries and, within a buffer zone of 3° from the northern and southern boundaries, the model temperature, salinity, and isopycnic surfaces are restored to the monthly ocean climatology, the Generalized Digital Environmental Model (GDEM), with an e-folding time scale of 5–60 days. It has a horizontal resolution of 1/12° (~5 km in the subpolar region) and 32 layers (with density referenced to 2000 m σ_2) in the vertical. Modeled surface fields are found to strongly resemble the mean dynamic topography in the study region (not shown). The model layers 25–29 correspond to the ISOW density range in the Iceland Basin with σ_2 values of 36.97 kg m^{-3}, 37.02 kg m^{-3}, 37.06 kg m^{-3}, 37.10 kg m^{-3}, and 37.17 kg m^{-3} (see Table 1 for details). For vertical/diapycnal mixing, the model uses the K-profile parameterization of Large et al. (1994). Further details about forcing formulation and horizontal mixing/diffusion parameters can be found in Xu et al. (2010, 2013).

The Atlantic simulations have been used previously to study the transports and spreading pathways of the Nordic Overflows in the Iceland and Irminger Basins (Xu et al., 2010, 2015, 2018; Lozier et al., 2022). In particular, as carefully documented in Xu et al. (2018), the model simulation reproduces the variability in volume transport with good agreement to the observational data collected at the CGFZ (Saunders, 1994; Bower and Furey, 2017). The simulation does tend to exhibit a deep bias within the ISOW layers as reported by Xu et al. (2010) who notes that modeled flow within the CGFZ is about 500 m deeper than observed. Regardless, because HYCOM has demonstrated good agreement with both observed transport magnitudes and spreading pathways, we consider it well suited to simulate the large-scale structure and variability of the ISOW layer for this study. We address and attempt to account for the depth bias when comparing modeled output to RAFOS float observations in Section 5.

2.1.1. Particle release experiment

To reconstruct ISOW spreading pathways from the Iceland Basin, simulated particle trajectories are generated based on OceanParcels or simply Parcels (https://parcels-code.org), a widely-used Lagrangian simulation framework for particle tracking, using daily mean outputs from the eddying HYCOM simulation. All particles are released from the eastern flank of the Reykjanes Ridge, north and south of the Bight Fracture Zone, along transects at approximately 58.5°N and 56.0°N (Fig. 2A). Each month for 540 months (January 1978–December 2022), 164 particles are released to total over 88,000 simulated particle trajectories within the ISOW layer. Particle trajectories are computed forwards in time for 10 years.

The two release locations were chosen to correspond to the deployment sites of RAFOS floats during the OSNAP campaign. The southern transect was included to intentionally exclude pathways that cross the Reykjanes Ridge and observationally target pathways to the CGFZ. While this approach introduces a small bias (<5%) in estimating the relative proportion of particles traveling along different pathways, results presented here were found to be largely insensitive to the choice to include or omit the particles from the southern release location. Therefore, particles from both locations are included in the analysis to ensure the most robust comparison to the RAFOS floats.

Particles used in this analysis are released where the time averaged velocity is southward (Fig. 2B) and within model layers 25 through 29 which coincide with σ_2 layers that make up ISOW at the release locations (Table 1). In the more commonly used σ_0 coordinates, this ranges from approximately 27.80 kg m^{-3} $\leq$ σ_0 $\leq$ 27.88 kg m^{-3}. We label and refer to these isopycnal layers by their model layer (25–29). The number of particles released each month within each layer decreases from 52 in layer 25 (shallowest layer) to 25 in layer 28 (Fig. 2B & C). In layer 29 (deepest layer), only 5 particles are released each month and so, for display purposes, these particles are sometimes excluded from figures however discussed when relevant. The number of particles released decreases in each layer because there is less ISOW flow in the deeper layers.

In this analysis, particles are classified by the pathway in which they leave the Iceland Basin, and by the direction they travel, east

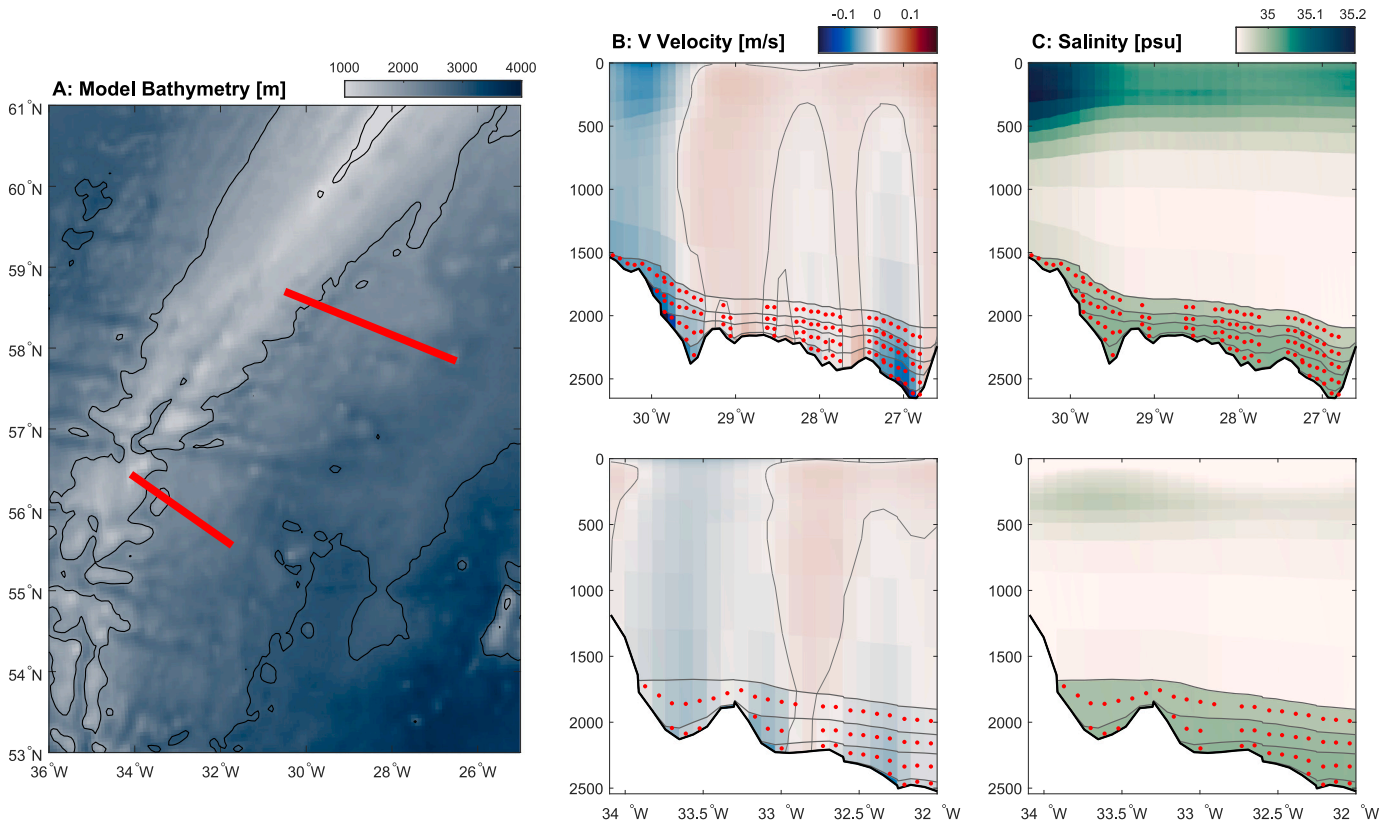

Fig. 2. Particle release locations and depths. (A) Locations where particles are released from are indicated in red and overlaid on model bathymetry. (B) Cross section of mean (1978–2022) meridional velocity and, (C) salinity, from north (top) and south (bottom) release locations. Black lines represent isopycnals of the ISOW layer and red dots indicate location and depths where particles are released. Gray contours indicate the time mean model isotach. Particles are released where the time average flow is southward.

Table 1
Summary of particle release parameters. Table lists the layer number, the corresponding σ_2 value, the approximate σ_0 value, the number of particles released each month and the approximate depth range at release site.

Layer Number	σ_2 [kg m^{-3}]	$\sim\sigma_0$ [kg m^{-3}]	Particles Released	Depth Range at Release [m]
25	36.97	27.78	52	1500 - 2250
26	37.02	27.82	45	1800 - 2350
27	37.06	27.84	37	2000 - 2400
28	37.10	27.87	25	2200 - 2500
29	37.17	27.89	5	2250 - 2650

vs. west, after leaving the CGFZ. To do this, we define a box around the CGFZ (Fig. 3: white) and gates along the axis of the Reykjanes Ridge, spanning approximately 53°N to 64°N, and one across 52°N east of the MAR (Fig. 3: purple and red/pink lines, respectively). Particles are considered to have left the Iceland Basin along one of these pathways if they cross the respective gate. For example, if a particle crosses the Reykjanes Ridge gate into the Irminger Sea, we consider it to have taken the Reykjanes Ridge pathway. However, a particle to travel through the CGFZ and into the Irminger Sea would not have taken the Reykjanes Ridge pathway. While it is typical for particles to cross the gates multiple times, nearly all particles subsequently travel into the Irminger Sea or WEB as opposed to returning to the Iceland Basin. Occasionally, particles cross the Reykjanes Ridge gate and travel southward into the CGFZ before entering the Irminger. These particles were classified as CGFZ particles.

To classify the direction particles travel from the CGFZ, a subset of particles that travel into the CGFZ is first created. This is done by considering a box around the CGFZ (52°N–53°N & 35°W–31.5°W) and including only those particles that traveled inside the box (Fig. 3: white box). The remainder of the domain is split into quadrants, east and west of the Reykjanes Ridge while north of 52°N and east and west of the Mid-Atlantic Ridge while south of 52°N. The number of days each particle spends in the western vs. eastern quadrants in the 600 days after leaving the CGFZ is then considered. If particles spend more than

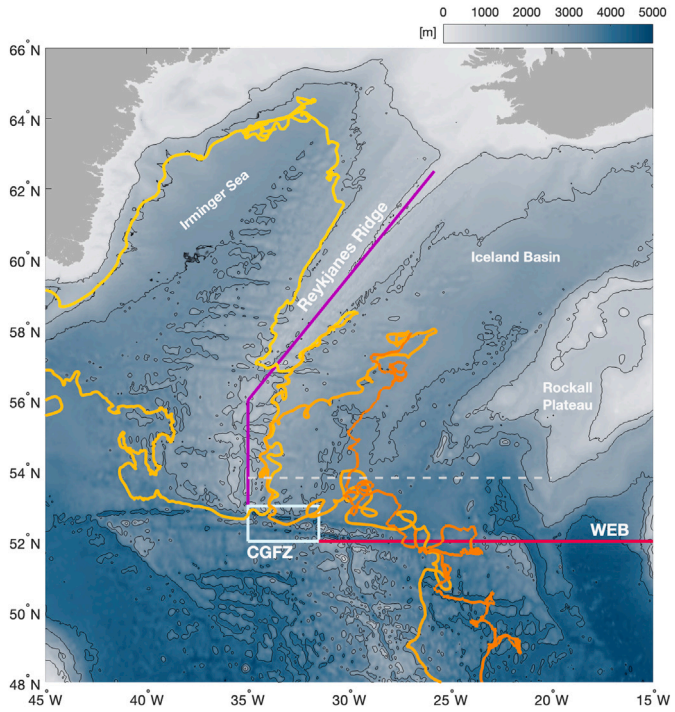

Fig. 3. Reykjanes Ridge (purple) and WEB (red/pink) gates along with CGFZ box (white) used to classify particle exit pathways from the Iceland Basin. Overlaid are examples of particle trajectories (yellow/orange). Bathymetry is plotted in the background and contoured every 1000 m. Dashed gray line identifies the section across which monthly volume transports are calculated in Section 3.1.

80% of those 600 days in either the eastern or western quadrants, they are assigned the corresponding direction. More than 90% of particles (that enter the CGFZ) were able to be classified by this condition.

Of the remaining 10% of particles, about half of them exhibited a characteristic loop-like behavior in which they completed a relatively slow, cyclonic trajectory from the western edge of the CGFZ before being swept back through the CGFZ and ultimately ending up in the eastern quadrants. These particles were given an east designation but they were few in number and their inclusion did not alter the results. It is possible this classification of particles mirrors RAFOS float behavior described by Zou et al. (2020) in which meanders of the NAC trap floats/particles and divert them southward. The remaining particles are considered inconclusive and excluded from the east vs. west analysis. Note that particles given a westward designation are considered to have exited the Iceland Basin via the CGFZ. On the other hand, particles given an eastward designation are still free to be exported either into the WEB or, less commonly, travel north and then over the Reykjanes Ridge.

2.2. RAFOS floats

In additional to the simulated particles, 40 acoustically tracked isobaric RAFOS floats (Rossby et al., 1986) are used to illustrate spreading pathways of ISOW out of the Iceland Basin. They are a subset of the 135 RAFOS floats deployed throughout the subpolar gyre between 2014 and 2017 (Ramsey et al., 2020) as part of the Subpolar North Atlantic Program (OSNAP). Here, we select for floats with a long enough lifespan to identify an exit pathway from the Iceland Basin. Floats were ballasted and deployed to track dense overflow waters that make up the lower part of the NADW and confirmed at launch to be embedded within the targeted isopyncal layer with shipboard CTD profiles. All OSNAP floats were deployed for two years and acoustically tracked underwater using an array of moored sound sources. They recorded daily measurements of pressure, temperature and acoustic times of arrival which, once converted to distance, were used to reconstruct the float trajectories upon surfacing.

The 40 RAFOS floats used here targeted the ISOW layer (1800–2800 m) and were deployed in three locations: within the CGFZ (~52.9°N) and along the eastern flank of the Reykjanes Ridge, just north and south of the Bight Fracture Zone (~56.0°N and ~58.5°N). RAFOS release locations are marked by solid red lines in Fig. 1. Three of the 40 floats used exhibited notable pressure drift, identified as a deviation larger than ±10 dbar upon surfacing. A linear correction was applied to the pressure records of the three floats. A number of floats, especially those that traveled through gaps in the Reykjanes Ridge, also exhibited missing tracks during their deployment lifetime. This was most commonly due to topographic blocking of sound signal but also frequently occurred during the winter months when sound propagation is reduced due to increased surface roughness. During these time periods, float positions are unknown but pressure records are still recovered.

2.3. World Ocean Atlas

The 2023 World Ocean Atlas (WOA) climatology is used here to estimate the along-track isopycnal from the RAFOS float pressure record. The WOA is a gridded climatological product of the World Ocean Database, the largest collection of publicly available ocean profile data. Here, the 2015–2022 climatology of temperature and salinity is used. This product is gridded on a quarter-degree horizontal grid at 102 standard depth levels.

3. Interannual variability in export pathways

To explore the interannual variability in ISOW spreading pathways, we calculate the percentage of particles to be exported along each pathway and evaluate fluctuations over the 40-year time period (Fig. 4). Particles are binned monthly by their release date to directly compare between export pathways. Additionally, particles are categorized according to the density layer they were released within. The following is a discussion of results presented in Fig. 4 and summarized in Fig. 14.

From the particle release experiment, it is apparent only the shallowest layers of ISOW (layers 25 & 26) are exported over the Reykjanes Ridge (Fig. 4A), presumably because denser layers are topographically blocked from traversing the ridge, a finding also documented by Xu et al. (2010) who use an earlier version of the same HYCOM simulation. Moored instrument observations from within the BFZ suggest however that ISOW with σ_0 as large as 27.85–27.87 kg m^{-3} (layers ~27–28; Table 1) can be found traversing the ridge (Furey et al., 2024), which is denser than the top two layers documented here. Given that the BFZ is the deepest passageway north of the CGFZ along the Reykjanes Ridge, observations within it likely capture the densest possible ISOW capable of crossing the ridge. When considering all fracture zones collectively, the limited export of dense ISOW through the BFZ may become negligible in an averaged sense. Additionally, the deep bias of the model may artificially depress ISOW layers while the 1/12° model bathymetry under-resolves the deepest extents of the fracture zones by 100–300 m (not shown). As a result, the modeled Reykjanes Ridge throughput may slightly under represent particle transport of the denser ISOW layers.

The percent of layer 25 particles released to be exported over the Reykjanes Ridge ranges from about 40% to just over 60% with a 40-year time mean of about 52% (Fig. 4A: turquoise). This represents about 16% of all particles released. The percent of layer 26 particles exported over the ridge ranges from about 5% to 25% with a 40-year time mean of about 13% (Fig. 4A: purple). This represents about 4% of all particles released. Together, about 20% of all particles released are exported over the Reykjanes Ridge (Fig. 4A: black). In both layers,

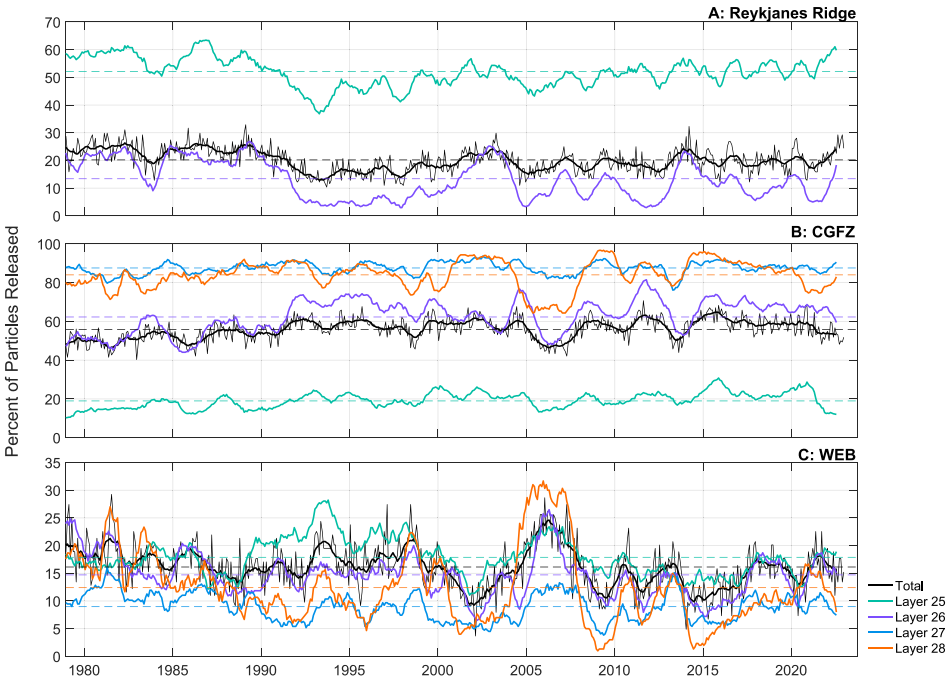

Fig. 4. Percent of simulated particles released to exit the Iceland Basin, (A) over the Reykjanes Ridge, (B) through the Charlie Gibbs Fracture Zone or (C) southward into the WEB. Colors indicate the isopycnal layer the particles were released within, where turquoise = layer 25, purple = layer 26, blue = layer 27 and orange/red = layer 28. Black represents the sum total over all the layers. Dashed lines indicate the time averaged percentage of particles to exit via each pathway. Time series are smoothed using a 12-month boxcar moving mean filter. In panel A, only particles from layers 25 and 26 crossed the ridge while deeper particles were blocked by the bathymetry. Note the sum totals in each panel (black) do not perfectly add up to 100% because a small number of particles stay within the Iceland Basin.

export is primarily dominated by a signal that varies on a timescale of about 5 years to decadal. The time period between 1980 and 1990 is characterized by above average export while the subsequent decade, 1990 to 2000, is characterized by below average export. Sustained lower than average export over the ridge is also found between 2005 and 2013. Large scale forcing of this interannual variability is discussed in Section 3.1.

As the CGFZ is much deeper than fracture zones along the Reykjanes Ridge, particles in every layer, except the deepest layer, are found to exit the Iceland Basin along this route (Fig. 4B). Similar to what has been reported by Xu et al. (2010) and others, the CGFZ is found to be the primary export pathway from the Iceland Basin as about ~55% of all particles take this pathway as compared to ~20% and ~16% for the Reykjanes Ridge and WEB respectively (Fig. 4: black lines). Export is largest in the deeper layers, 27 and 28, which both on average have export percentages larger than 80% and together account for over 40% of the total number of particles. About 60% of particles released in layer 26 are exported through the CGFZ while only about 20% of particles in layer 25 take this pathway out of the Iceland Basin (about 16% and 6% of total respectively). The lower throughput in the upper layers is due, in part, to the significant percentage of upper layer particles to travel over the Reykjanes Ridge. Additionally, in Section 3.2 we will show that the eastward flowing NAC preferentially deflects these upper layer particles away from the CGFZ.

Particle export through the CGFZ appears to have slightly higher temporal variability and varies on a time scale of about 2.5–5 years. In layer 26, the period of time between 1980 and 1990 is characterized by lower CGFZ export compared to above average export between 1990 and 2000, an anticorrelation to export over the Reykjanes Ridge. In other words, when export over the Reykjanes Ridge is elevated (reduced), a smaller (larger) percentage of particles is able to propagate south to the CGFZ. This pattern is also observed in layer 25, albeit less striking. The most notable feature in the CGFZ time series however is a significant decrease in particle export between 2005 and 2008. This sharp decrease in export occurs in every layer but is most pronounced in layers 26 and 28. Additionally, a slight long-term increasing trend in CGFZ export is also noticeable in the time series, though it is not quantified here and its statistical significance remains unclear. Large scale forcing of this interannual variability is discussed in Section 3.2.

Particle export into the WEB is consistent between each layer illustrated in Fig. 4C. Time mean WEB export ranges from about 10% (layer 27) to about 17% (layer 25) and accounts for near 17% of the total particles released. The time series present a high degree of correlation between layers. The large decrease in CGFZ export between 2005 and 2008 is reflected as a large increase in WEB export, suggesting that particles deflected eastward away from the CGFZ are more likely to end up in the WEB. Additionally, corresponding to the long-term trend in CGFZ export, WEB export appears to decrease in every layer throughout the time series. This anticorrelation between CGFZ and WEB export is in agreement with Zou et al. (2017) who, using the Family of Linked Atlantic Models Experiment (FLAME), note that when cumulative ISOW export across both Reykjanes Ridge and CGFZ is strong, export into the WEB is relatively weak. Nearly all layer 29 particles are exported into the WEB (not shown but discussed in Section 4).

3.1. Controls on interannual variability over the Reykjanes Ridge

While deep Argo and RAFOS floats have been used to document ISOW pathways through gaps in the Reykjanes Ridge, there exists only a single long term mooring array that has measured the temporal variability of ISOW transport through the ridge. Using data from these two moorings in the BFZ, Furey et al. (2024) identified a strong seasonal cycle with enhanced westward transport in the summer/fall and weakened, or sometimes reversed, transport in the winter/spring months. Seasonal fluctuations could not be correlated with sea surface height differences across the fracture zone, a proxy for geostrophic pressure gradients that can drive along-isopycnal flow, and therefore the forcing of cross-Reykjanes Ridge transport remains unknown. We

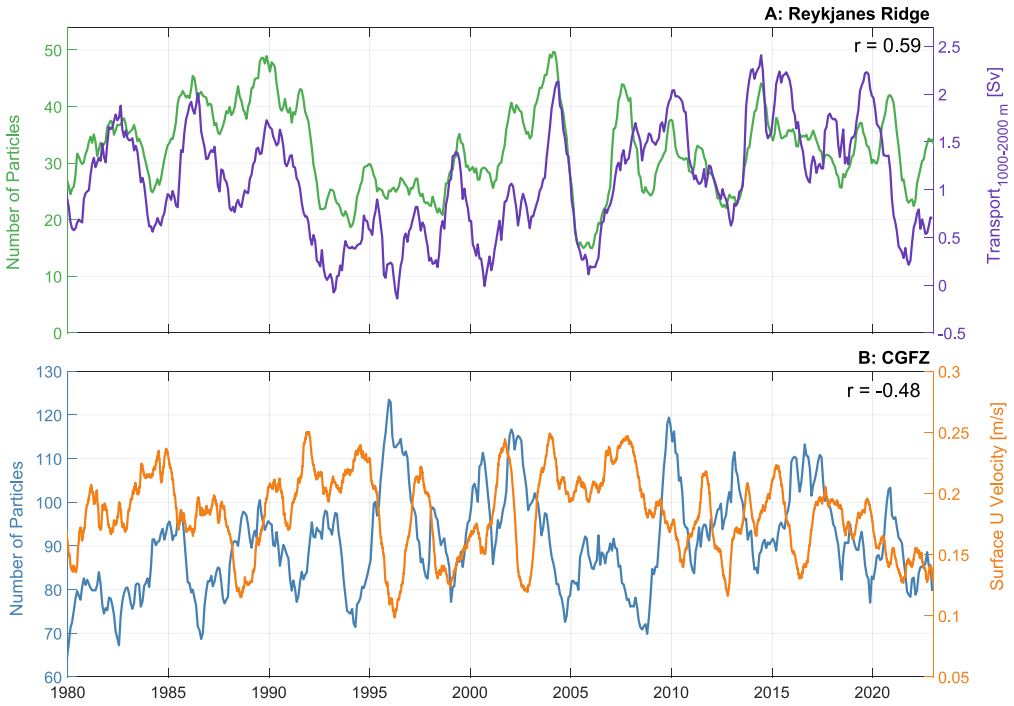

Fig. 5. Controls on particle export over the Reykjanes Ridge (A) and through the CGFZ (B). (A) Number of particles exported from the Iceland Basin to travel over the Reykjanes Ridge (green) compared transport across 53.80°N between 1000–2000 m depth. The number of particles only includes those from layer 25 & 26 and are binned monthly by their initial cross date over the Reykjanes Ridge gate. Transports are calculated from monthly HYCOM outputs. (B) Number of particles that are deflected westward from the CGFZ (blue) vs. the zonal surface velocity averaged within the CGFZ (orange). The number of particles represents all layers collectively. Zonal velocities are calculated from daily HYCOM outputs. All time series are smoothed using a 12-month boxcar moving mean filter.

explore this question from a Lagrangian reference frame by considering the number of particles to be exported over the Reykjanes Ridge each month. Here, particles are binned by the month they cross over the Reykjanes Ridge gate, rather than by their release date, and compared against monthly mean HYCOM output. While we previously binned by release month to compare between each of the exit pathways, the choice to now bin by month of crossing assures minimal lag between forcing and response.

We find that the number of particles to be exported over the Reykjanes Ridge is strongly correlated ($r = 0.59$, $p < 0.001$) to northward volume transport into the Iceland Basin, across 53.80°N (Fig. 5A). To arrive at this transport estimate, a section along 53.80°N is created between the Reykjanes Ridge (35°W) and the Rockall Plateau (20°W; Fig. 3 dashed gray line). Monthly mean volume transports are derived between the depth range of 1000–2000 m. This depth range was chosen to correspond to the depth range in which ISOW is forced over and through gaps in the Reykjanes Ridge however a similarly strong correlation is identified by isolating transport within the upper two isopycnal layers of ISOW (layer 25 and 26; not shown).

The high correlation suggests that a stronger NAC, which primarily carries upper layer waters, penetrates well below the thermocline and additionally increases the volume of intermediate and deep waters occupying the basin interior. Mean intermediate depth circulation across the 53.80°N line includes a weak but persistent northeastward flow, consistent with the upper layer circulation, which contrasts the predominantly southward mean flow down the eastern flank of the Reykjanes Ridge (Bower et al., 2002). As such, an intensified NAC, represented by larger northward transports into the Iceland Basin, enhances the northeastward transport of intermediate and deep waters into the basin. The Reykjanes Ridge serves as the primary exit pathway for ISOW at these depths, and so an increase in inflow is balanced by stronger export across the ridge. The relationship reflects the basin-scale adjustment to changes in intermediate-depth inflow, with the ridge acting as a dynamic choke point modulating the westward spread of ISOW. We recognize this simple box-model does not capture the influx of dense overflow water entering the basin via the sills however observations suggest this inflow is comparatively steady in time (Hansen and Østerhus, 2007; Hansen et al., 2016) and variability in the 1000–2000 m layer is therefore more strongly tied to NAC dynamics.

3.2. Controls on interannual variability within the CGFZ

As the primary exit pathway of ISOW from the Iceland Basin, deep westward flow through the CGFZ and interaction with the strongly barotropic eastward NAC has received a significant amount of attention in recent years. Using two years of data from a mooring array in the CGFZ, Bower and Furey (2017) demonstrates that strong northward meanders of the NAC weaken ISOW transport through the CGFZ and can even lead to eastward reversals of the deep flow. Zou et al. (2017) provides additional Lagrangian insight using particles seeded within a high resolution numerical model to illustrate a strong anticorrelation on semi-decadal timescales between westward ISOW export through the CGFZ and southward ISOW export to the WEB. Here, we build on this Lagrangian framework by extending the analysis to our 40-year time series, allowing for a more comprehensive assessment of the robustness and variability of this relationship.

The number of particles to successfully transit westward through the CGFZ is compared against zonal sea surface velocity averaged within the CGFZ (Fig. 5B). Obtained from daily mean HYCOM output, zonal sea surface velocity is found to be the best proxy for the meridional displacement of the NAC within the CGFZ such that a larger U velocity represents a more northward shift of the zonally oriented NAC. Here, particles are again binned monthly by their arrival date into the CGFZ to most closely align with HYCOM output. A moderate-to-strong anticorrelation is observed ($r = -0.48$, $p < 0.001$), reinforcing the viewpoint that ISOW can be blocked and ultimately remain east of the Reykjanes Ridge or MAR when the NAC advances northward. The anticorrelation

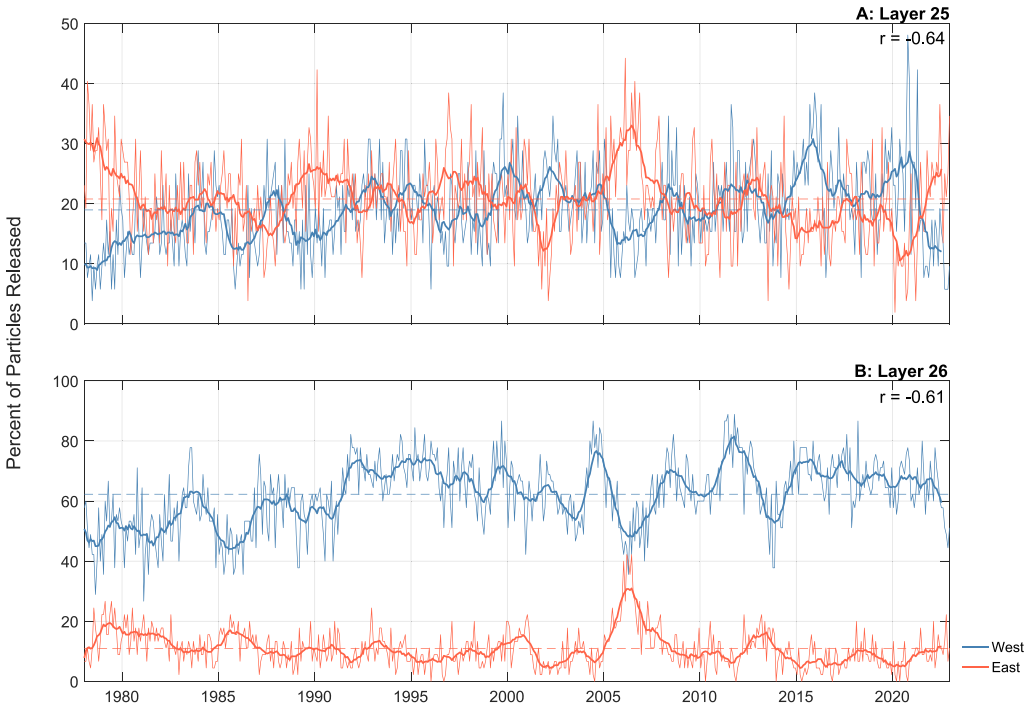

Fig. 6. Percent of simulated particles released to successfully exit the Iceland Basin through the Charlie Gibbs Fracture Zone (western export, blue lines) vs. those that are deflected eastward (red lines) after entering the CGFZ in layer 25 (top) and layer 26 (bottom). Time series are smoothed using a 12-month boxcar moving mean filter and plotted on top of the monthly time series.

is not as strong as the correlation between Reykjanes Ridge export and transport into the Iceland Basin (Fig. 5A) likely due, in part, to the fact that export through the CGFZ will depend not only on the position of the NAC but also on the number of particles that are able to successfully transit south from the Reykjanes Ridge. If a large number of particles are being exported over the Reykjanes Ridge, fewer particles will be available to cross the CGFZ.

In Fig. 6, the percent of particles released, binned monthly by their release date, to be exported westward from the Iceland Basin via the CGFZ is compared against the percent of particles to enter the CGFZ and ultimately end up in the eastern basin. Note this is accomplished by classifying particles within the CGFZ, white box in Fig. 3, and their subsequent pathways. Particles to end up east of the CGFZ are assumed to have been blocked from translating through the fracture zone by a northward positioned NAC. The goal of this analysis is to determine if the percentage of particles to end up in the eastern basin is anticorrelated with the percentage of particles to end up in the western basin. This is a modification to the approach of Zou et al. (2017) who compare CGFZ export directly to WEB export. The distinction is made here to account for the fact that (1) a number of particles take a direct southward route to the WEB without interacting with the NAC in the CGFZ (Fig. 3) and (2) particles deflected eastward from the CGFZ do not unanimously end up in the WEB and can instead recirculate in the Iceland Basin (see Section 4.1).

The percentages of particles to end up east versus west of the CGFZ are compared in layer 25 (Fig. 6A) and layer 26 (Fig. 6B). A strong anticorrelation is observed in both layers ($r_{25} = -0.64$, $r_{26} = -0.61$, $p < 0.001$) such that when more particles end up east of the Reykjanes Ridge and MAR, fewer particles are being exported through the CGFZ and vice versa. On average, in layer 25, the percent of particles being exported via the CGFZ and the percent of particles remaining in the eastern basin both vary around 20%. In layer 26 however, the percentage of exported particles varies around 60% while only about 10% of particles travel eastward from the CGFZ. In the deeper layers (not shown), on average less than 5% of particles travel eastward, suggesting that the influence of the NAC is largely confined to the upper layers of ISOW and the eastward flowing current may not be barotropic enough to influence the densest overflow waters.

An exception to this depth dependency is identified at a few time periods, namely 2006 and 2013, when the influence of the NAC is felt throughout the water column and eastward export peaks above 20% in every layer. In all but layer 25, these peaks are far outside the range of typical variability. The deep reaching influence of the NAC during these time periods is attributed to an exceedingly northward position that centers the core of the northernmost branch of the current directly over the northern CGFZ for an extended period of time.

4. Depth-dependence in export pathways

The above findings illustrate that the Iceland–Scotland Overflow should not be treated as a single homogeneous layer and that exit pathways, and the ultimate fate of particles, is strongly dependent on depth and density within the ISOW layer. To further explore this depth dependency, probability distribution maps are generated using the 10-year simulated particle trajectories, split into respective layers (Fig. 7). These probability distribution maps represent the percentage of particle positions such that the total value of all grid cells (1/4°) collectively, adds up to 100%.

In layer 25 (Fig. 7A), the majority of particles travel through gaps in the Reykjanes Ridge, consistent with Fig. 4. The BFZ and, further south, the no-name gap (~55°N) appear to be the primary conduits for these particles however some do travel over and within other channels in the ridge. Upon entering the Irminger Sea, particles preferentially travel along the periphery of the basin, within the deep boundary current, and continue on into the Labrador Sea. Very few particles appear to successfully traverse the CGFZ and connectivity to the outflow at the northern fracture zones appears weak. Of the particles that remain east of the ridge systems, a larger portion penetrate back into the Iceland Basin as compared to the deeper layers. Southward spreading into the WEB is also observed.

In layer 26 (Fig. 7B), some particles still pass through the BFZ and no-name gap but the majority of particles appear to travel through

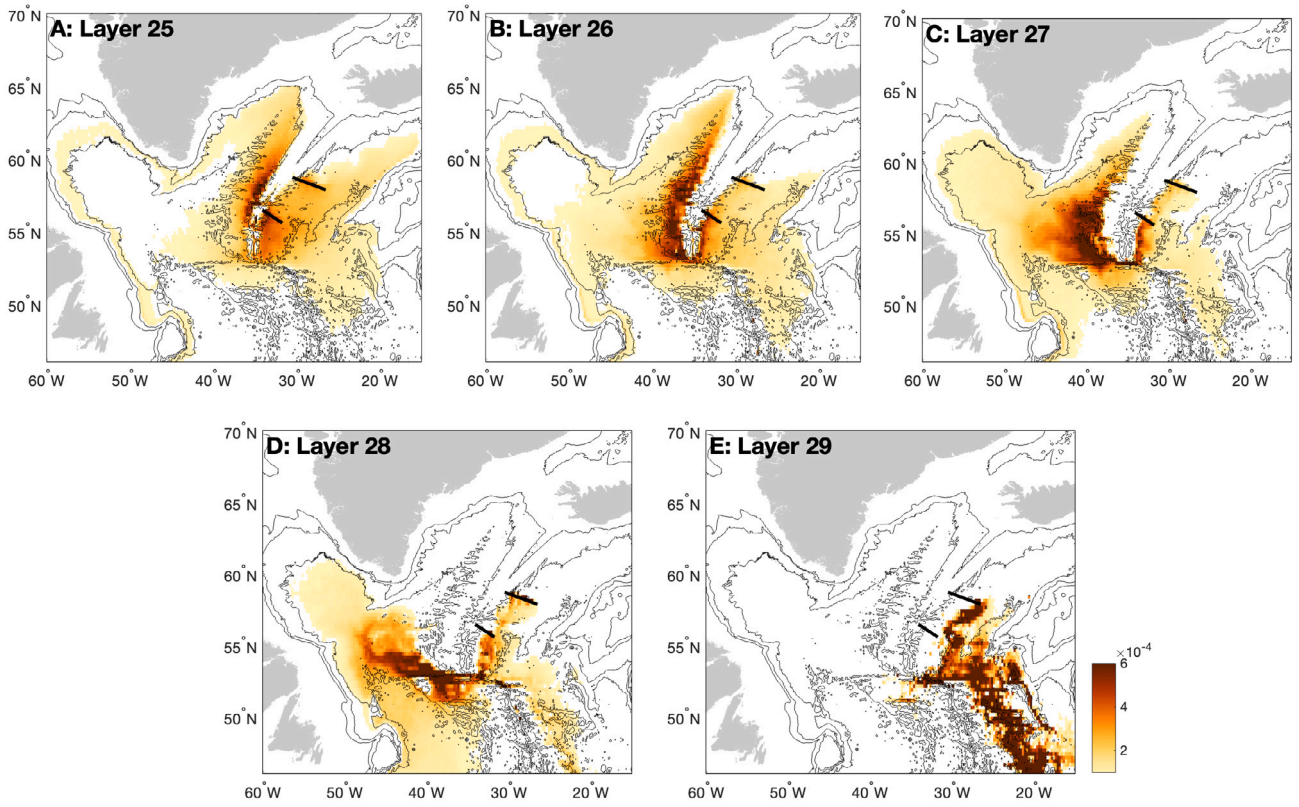

Fig. 7. Probability distributions of 10-year simulated particle trajectories after initialization at two locations (~58°N and ~56°N) along the eastern flank of the Reykjanes Ridge in (A) layer 25, (B) layer 26, (C) layer 27, (D) layer 28 and (E) Layer 29. Black lines indicate particle release sites. Bathymetry is contoured every 1000 m.

the CGFZ and continue northward into the Irminger Sea as a deep boundary current. This boundary current from the CGFZ, occupying a depth range between the 2000 and 3000 meter isobath, embodies the traditional pathway of ISOW once exported from the Iceland Basin. On the eastern side of the ridge systems, WEB penetration appears slightly more common and extends further southward as compared to the upper-most layer while recirculation within the Iceland Basin is reduced.

In the deeper layers, 27 and 28 (Fig. 7C & D respectively), significant deviations from traditional pathways are observed. All westward export is through the CGFZ however particles subsequently travel northwestward towards the Southern tip of Greenland and Labrador Sea. In layer 27, this pathway is somewhat diffusive and particles can end up in either the Irminger or Labrador Sea however, in layer 28, particles are much more concentrated and take a direct path towards the Labrador Sea. It is likely that these deeper layers therefore provide a much more direct and less mixed supply of ISOW to the Labrador Sea. Whatever does not end up in the Labrador Sea appears to deflect southward, contributing to the deep western boundary current around the Flemish Cap and spilling into the Northwest Corner region. East of the ridge systems, particle behavior is similar in both layers. Particles are confined to the boundary current on the east side of the Reykjanes Ridge before translating southward into the WEB. It appears these deeper layers do not contribute to recirculation within the Iceland Basin.

In layer 29 (Fig. 7E), the deepest layer, nearly all particles are exported to the WEB. Because particles in this layer are deployed the furthest from the Reykjanes Ridge, many take a direct route into the WEB without interacting with the CGFZ. Those that do, typically cannot travel westward through the fracture zone, presumably because they are too deep. These particles tend to be exported into the WEB but there may also be some tendency to recirculate within the Iceland Basin, traveling northward from the WEB gate. In rare instances, layer 29 particles do successfully traverse the CGFZ and appear to preferentially travel southward from the fracture zone, although the number of particles is too small to draw any conclusions.

4.1. Fate of ISOW from the CGFZ

Particle distribution maps are further decomposed by considering only the particles that travel into the CGFZ and comparing westward vs. eastward propagation from the fracture zone (Fig. 8 left vs. right column). Maps are once again separated by layer of particle release. West of the CGFZ, pathways largely reflect those illustrated in Fig. 7. Namely, shallower layers tend to follow the boundary current into the Irminger Sea while deeper layers take a more direct path towards the Labrador Sea. The exception is in layer 25, which is quite distinct from its Fig. 7 counterpart because we are now excluding particles that traveled through gaps in the Reykjanes Ridge. The remaining particles, of which a much higher percentage originate from south of the BFZ release location, travel as a fairly diffuse (compared to deeper layers) boundary current along the eastern flank of the Reykjanes Ridge and eventually through the CGFZ. Upon exiting the fracture zone, particles appear to radiate both westward and northward and are notably more diffuse than the cohesive group that propagate northward in layer 26.

Particles that end up east of the ridge systems (Fig. 8: right column) typically propagate southward along the eastern flank of the Reykjanes Ridge into the CGFZ and are subsequently deflected by the deep reaching NAC. Previous work has suggested a significant portion of these particles end up propagating southward from the CGFZ into the WEB (Zou et al., 2017). Here, this pathway is identified in the deeper layers however, upper layers appear more likely to travel northward and recirculate within the Iceland Basin. In layer 25, a very dense cloud of high probability is found centered near 55°N, 30°W, suggesting

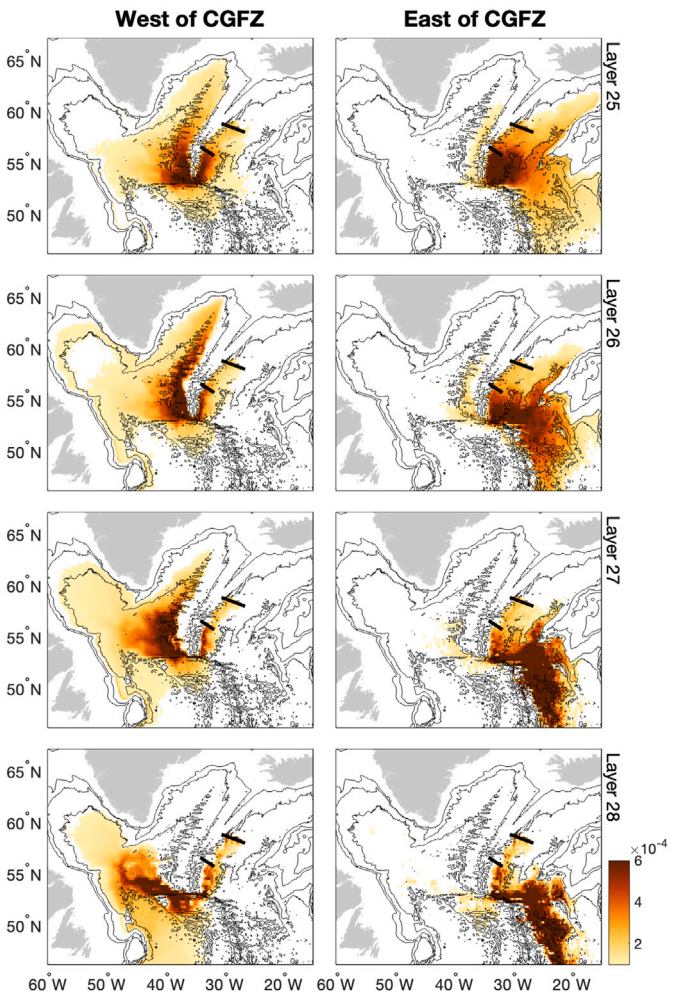

Fig. 8. Probability distributions of 10-year simulated particle trajectories that traverse the Charlie Gibbs Fracture Zone after being initialized at two locations (~58°N and ~56°N) along the eastern flank of the Reykjanes Ridge. The left column illustrates particles that propagate westward from the CGFZ and the right column illustrates particles that propagate eastward from the CGFZ. Each row represents the model layer particles were released within, from layer 25 in the top row to layer 28 in the bottom row. Black lines indicate particle release sites. Bathymetry is contoured every 1000 m.

particles are deflected northeastward and become concentrated in this region. From here, particles evenly radiate in all directions. Some particles recirculate, spreading northward into the Iceland Basin, likely carried by the energetic and deep reaching NAC which can interact with these upper layers of ISOW. Alternatively, the remainder spread further east and/or south into the WEB but remain fairly diffuse and span the whole region from east of the MAR to the edge of the domain.

In layer 26, particles seem to be deflected directly eastward from the CGFZ along ~55°N. While a small percentage of particles propagate north from here, concentrated along the northwest edge of the Rockall Plateau, the majority travel southward into the WEB. Moving towards deeper layers, the more concentrated the WEB particles become, banking up against the eastern flank of the MAR. In layer 28, there is no evidence for northward spreading and nearly all particles deflected eastward from the CGFZ end up in the WEB. In the deepest layer, nearly all particles stay east of the CGFZ and so the probability distribution map closely resembles Fig. 7E and is therefore omitted.

5. Comparison to RAFOS float trajectories

RAFOS floats deployed during OSNAP field campaigns in the years between 2014 and 2017 are used to observationally validate a depth dependency in ISOW layers. While this is a useful exercise to evaluate if model results resemble reality, we caution that a direct comparison is difficult because the observations are limited in number and lifespan.

In the following figures (Figs. 9, 10, 11 & 12), RAFOS trajectories are overlaid on contours of smoothed particle distribution maps (Figs. 7 & 8). Pressure records corresponding to the RAFOS trajectories are displayed below each map. During the times when RAFOS coordinates are available, the time average density at that location and pressure is determined from the World Ocean Atlas (WOA) climatology, and plotted in color on top of the pressure record. We use the WOA, as opposed to HYCOM, because of the deep bias identified in HYCOM. When comparing the two, isopycnal layers of ISOW within the time averaged HYCOM output are found to be about 100–500 m deeper than in WOA, with the largest discrepancy observed in the WEB and east of the MAR. This deep bias results in RAFOS trajectories artificially appearing to leave the ISOW layer in HYCOM.

To compare against the particle distribution maps, floats are grouped by their isopycnal layer. This was done systematically, according to the density class in which the float is associated with during the middle and end of its lifespan. The isopycnal at deployment, and shortly thereafter, is largely ignored because many floats initially transition from denser to lighter isopycnals within the ISOW layer. This occurs as isopycnals slope and converge against the ridge where floats were released. Additionally, our primary interest lies in float behavior after it has moved away from the eastern flank of the ridge and throughout its trajectory, as this provides the most direct comparison to particle behavior. We also note that because RAFOS floats do not measure salinity, isopycnal classification is inherently imperfect, and it is possible that some floats categorized within one density class may exhibit behavior more characteristic of an adjacent layer.

Overall, float trajectories compare exceptionally well with particle distribution maps. Of the ten floats to cross the Reykjanes Ridge, five are associated with layer 25 (Fig. 9A) and crossings are concentrated near the BFZ and no-name gap. Upon entering the Irminger Sea, three floats propagate northward along the western flank of the Reykjanes Ridge. These floats end up more centralized within the Irminger Sea than the highest particle distribution, which is banked up against the ridge, however the agreement is still significant. The remaining two floats (1351 & 1355) that crossed the ridge propagate southward which is a more uncommon pathway for the particles to take. Only a single float (1434) grouped in layer 25 traveled west from the CGFZ and immediately deflected northward along the ridge (Fig. 9B).

Six floats traveled east from the CGFZ (Fig. 9C). Comparison of float trajectories with SSH fields (not shown) indicate the NAC was in a more northern position when the floats were within the CGFZ, resulting in a large number traveling east from the fracture zone. Two (1401 & 1397) are rapidly deflected to the northeast, in close alignment with the particle distribution, while the remainders travel eastward before eventually ending up in either the WEB or recirculating within the Iceland Basin. All four remain in regions where particle distribution is still relatively high.

The remaining five floats to travel through gaps in the Reykjanes Ridge all correspond to layer 26 (Fig. 10A). Degraded float tracks do not allow concrete assessment of where floats cross, but it appears from the locations just prior to and after leaving the ridge, that two floats (1396 & 1310) cross at the BFZ, one (1311) crosses at the no-name gap and the remaining two floats (1441 & 1431) cross somewhere between. All of the floats that cross the ridge in this layer propagate northward upon entering the Irminger, in very close agreement with the particle distribution map. Three floats in this layer successfully translate through the CGFZ and while two (1435 & 1357) predictably deflect northward in good agreement with the particle distribution, the

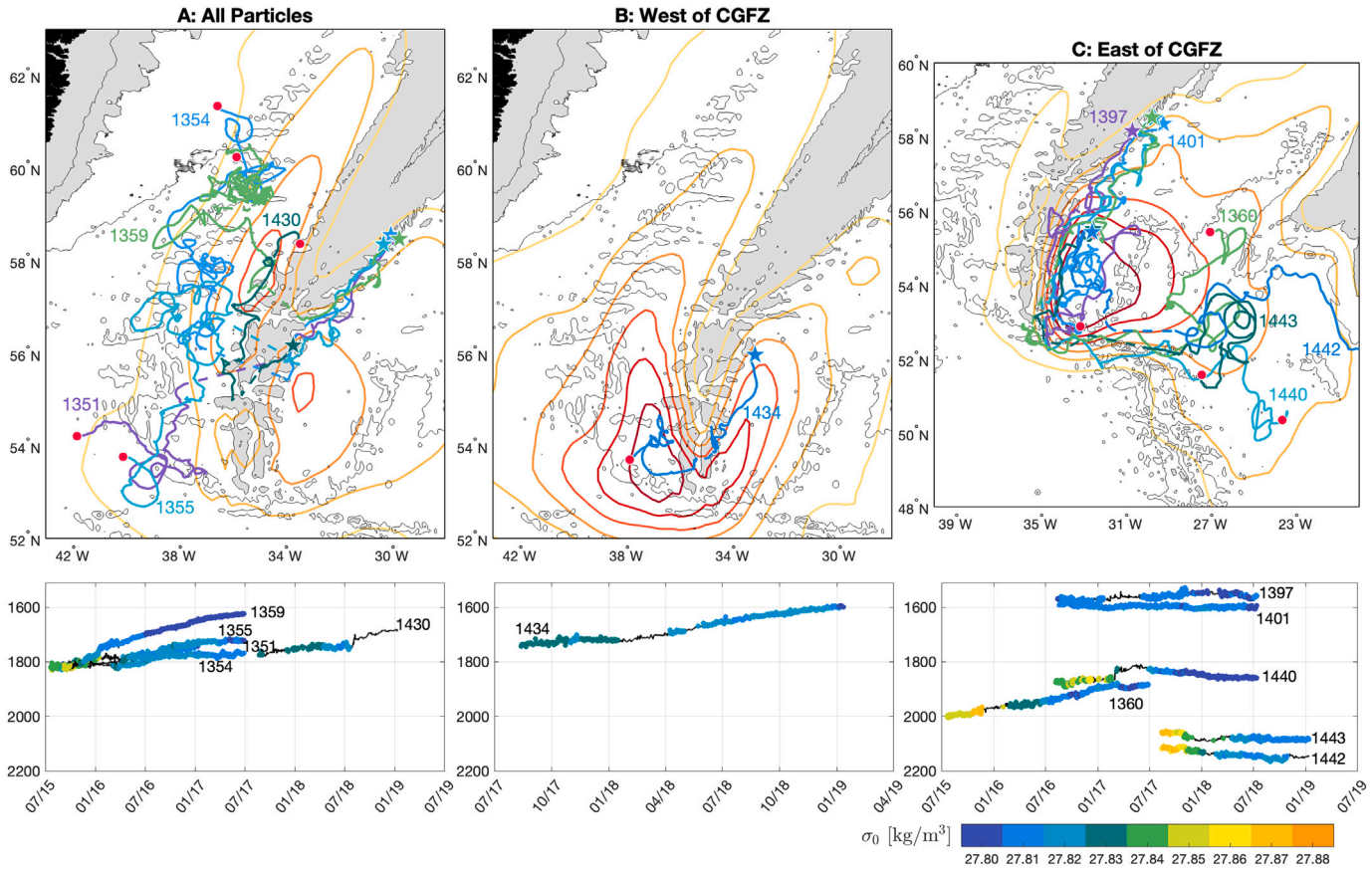

Fig. 9. Top: RAFOS float trajectories overlaid on layer 25 particle distribution contour maps. Bottom: RAFOS along track pressure colored by isopyncal layer determined from the World Ocean Atlas. Only the RAFOS floats occupying the shallowest density ranges (on average 27.8 and 27.82 kg m^{-3}) are included. Sections of the float trajectories in dashed lines are times when coordinates could not be recovered and correspond to the time periods where pressure records are not colored. Stars indicate the initial float position and red circles indicate final float position. Trajectories and corresponding pressure records are labeled by RAFOS float serial number. From left to right (A to C) are particle distribution maps of all particles released within layer 25, particles that travel west from the CGFZ and particles that travel east from the CGFZ, respectively. Bathymetery shallower than 2000 m is colored in gray and the 1000, 2000 and 3000 meter isobaths are contoured on top.

remaining float (1379) propagates southward before heading northwest (Fig. 10A). This does not appear to be outside the range of possible particle pathways however is much less common. Seven floats remain east of the CGFZ in layer 26 (Fig. 10B) and all are in fairly good agreement with the particle distribution, translating eastward from the CGFZ before propagating either north or south. Note, a single float (1436) traveled directly south from its release location without being deflected from the CGFZ. This is not directly comparable to the particle distribution map because it does not interact with the CGFZ however because it ultimately ends up where particle distribution is highest we felt it was an interesting case to include.

As a group, floats in layer 27 have the weakest agreement with the particle distribution maps. Four floats propagate west from the CGFZ (Fig. 11A) and while one (1322) takes a fairly predictable northwestward pathway that is in good agreement with the particles, the remainder travel southward from the CGFZ. While this is not outside the range of what the particles predict, it appears much more common in the float trajectories suggesting the model may not accurately capture this southward propagation pathway from the CGFZ. East of the CGFZ, four floats all exhibit quite different behavior from each other (Fig. 11B). One float (1410), released closer to the center of the basin, does not appear to get trapped within the southward boundary current, taking an indirect meandering route to the CGFZ before ending up in the region of highest particle distribution at the end of its lifespan. Another float (1439) went northward from the CGFZ while the other two (1369 & 1403) went southeastward before translating back over the MAR and into the western basin. Longer float lifespans could have better resolved some of these pathways however the overall lack of agreement in this layer is puzzling.

Layer 28 floats exhibit remarkable agreement to the particle distribution map (Fig. 12), especially in comparison to the previous layer. Of the four floats identified in this layer, three were launched from the CGFZ while the remainder was launched from north of the BFZ on the eastern flank of the Reykjanes Ridge. All traveled in a northwest direction from the CGFZ and a single float (1338) propagated so far northward it surfaced remarkably close to the Labrador Sea. No floats in this layer traveled east from the CGFZ, which is unsurprising given that earlier results indicate only sustained, far-reaching northward intrusions of the NAC can impact these deeper layers.

A previous finding from the OSNAP program, largely based on data from the same RAFOS floats used here, is that the so-called 'traditional' ISOW pathway out of the Iceland Basin, namely through the CGFZ and northward along the western flank of the Reykjanes Ridge (Dickson and Brown, 1994; Schott et al., 1999), was not observed in the float trajectories (with one exception) and is more of the exception rather than the typical pathway (Zou et al., 2020; Lozier et al., 2022). The depth dependence observed here helps to reconcile this understanding. We have shown that only particles in the shallowest layers of ISOW take this traditional pathway, however these are also the layers where particles are most susceptible to crossing the Reykjanes Ridge north of the CGFZ or being deflected by the NAC. As a result, many particles and floats have already taken alternative routes by the time they reach

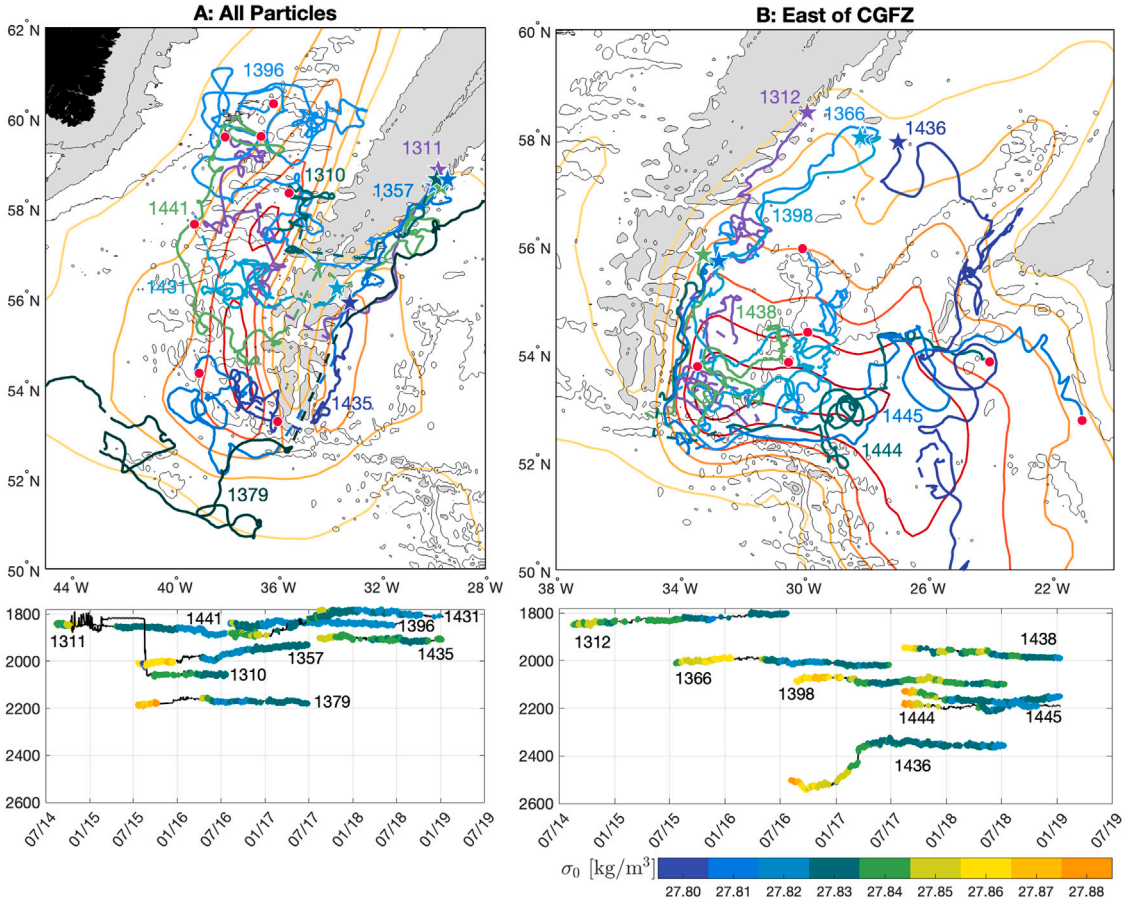

Fig. 10. Same as Fig. 9 except particle distribution maps are for layer 26 and RAFOS float trajectories occupy a density range of, approximately, between 27.82–27.84 kg m^{-3}.

the CGFZ. While a few floats in layer 25 and 26 do turn northward at the CGFZ, their limited lifespan prevents conclusive determination of their ultimate fate. It is possible that shallower floats deployed from the CGFZ might have more thoroughly documented the traditional ISOW pathway however most of these floats were deployed within the densest ISOW layers.

While float behavior is largely in agreement with simulated particle trajectories, there are a few pathways that seem well documented by the floats and less resolved by the model. Namely, southward propagation west of the MAR from the CGFZ, and an east-to-west pathway through the MAR. Documented by Zou et al. (2020), around five floats travel south from the CGFZ and, while none travel outside the range of particle pathways, it appears far less common in the model. Zou et al. (2020) suggests this southward deflection could be associated with meanders in the deep-reaching NAC that act to envelop floats and draw them southward. It is therefore possible that a specific configuration of the NAC when the floats were present resulted in a higher percentage of floats being forced southward than might otherwise be expected. It is however interesting to note that the majority of floats to demonstrate this behavior are deeper than we might expect to feel the influence of the NAC.

6. Discussion and conclusions

In this study, daily mean HYCOM output is used to simulate particle trajectories within ISOW layers of the Iceland Basin. More than 88,000 particles are used to explore the interannual variability in export pathways as well as the depth dependence within the ISOW layer itself. This work builds on previous studies that have identified the primary ISOW export pathways, including those over the Reykjanes Ridge, through the Charlie Gibbs Fracture Zone, and into the Western European Basin (Xu et al., 2010; Zou et al., 2020; Lozier et al., 2022). Here, we further explore these three pathways using Lagrangian particle tracking and diagnose the large-scale forcing associated with each route.

Export over the Reykjanes Ridge is shown to vary on time scales from about 5 years to decadal, with sustained maximum export between 1980 and 1990 and sustained minimum export between 1990 and 2000 (Fig. 5A). We find that Reykjanes Ridge export is closely linked to transport into the Iceland Basin between the depth range of 1000–2000 m suggesting that a strong NAC results in more westward export over the ridge. This relationship points to a large-scale dynamic control, likely tied to variations in the strength, size and structure of the subpolar gyre.

We hypothesize that the transport variability into the Iceland Basin, and consequently the export of ISOW over the Reykjanes Ridge, is associated with a spin-up of the subpolar gyre, dynamically linked to both its strength and spatial extent. During a spin-up, the gyre expands to its largest extent, characterized by an increased area enclosed by the outermost SSH contour and a steepened SSH gradient between the gyre interior and its periphery. This results in stronger cyclonic circulation, increased northward flow of the NAC and is accompanied by a lowered SSH in the basin interior. Foukal and Lozier (2017) assessed subpolar gyre variability using these metrics and found that much of the interannual and seasonal variability in gyre area is expressed in the northeastward extent in the Iceland Basin. They identified a clear seasonal cycle, with gyre spin-up in the fall and spin-down in the spring, consistent with transport measurements through the Bight Fracture Zone reported by Furey et al. (2024). Additionally, Foukal and Lozier (2017) documented interannual variability in gyre area on

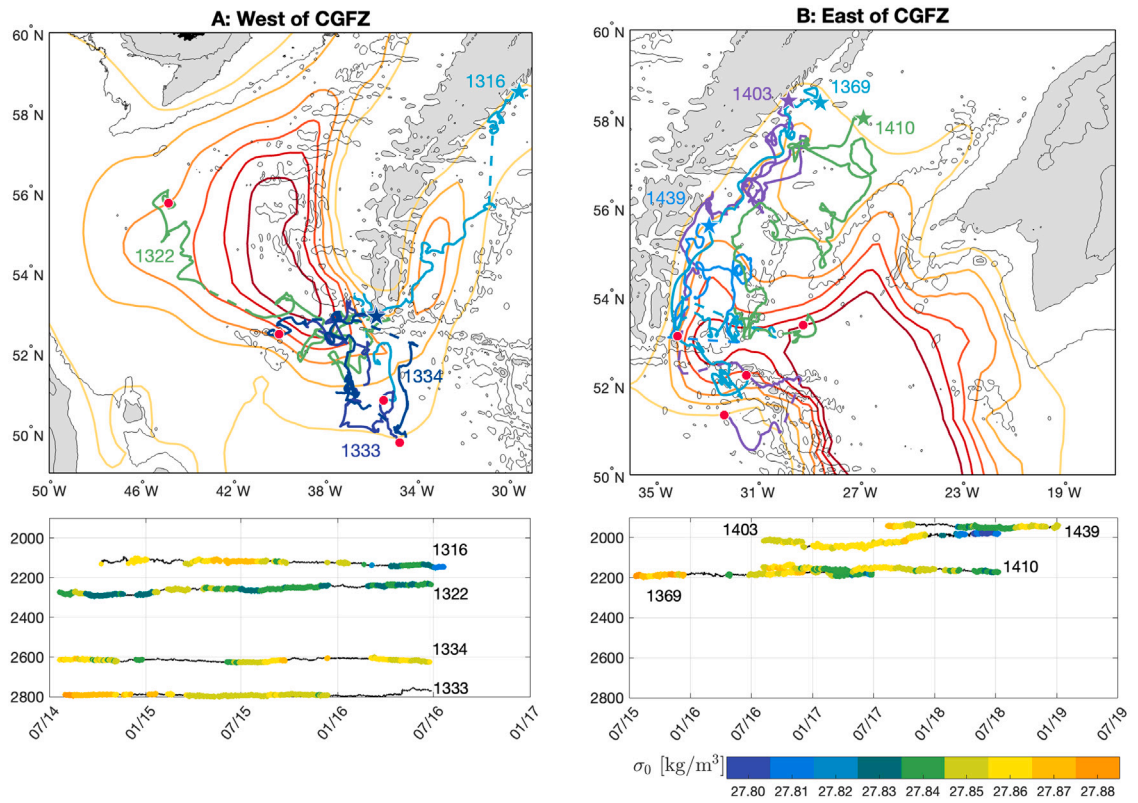

Fig. 11. Same as Fig. 9 except particle distribution maps are for layer 27 and RAFOS float trajectories occupy a density range of, approximately, between 27.84–27.86 kg m^{-3}.

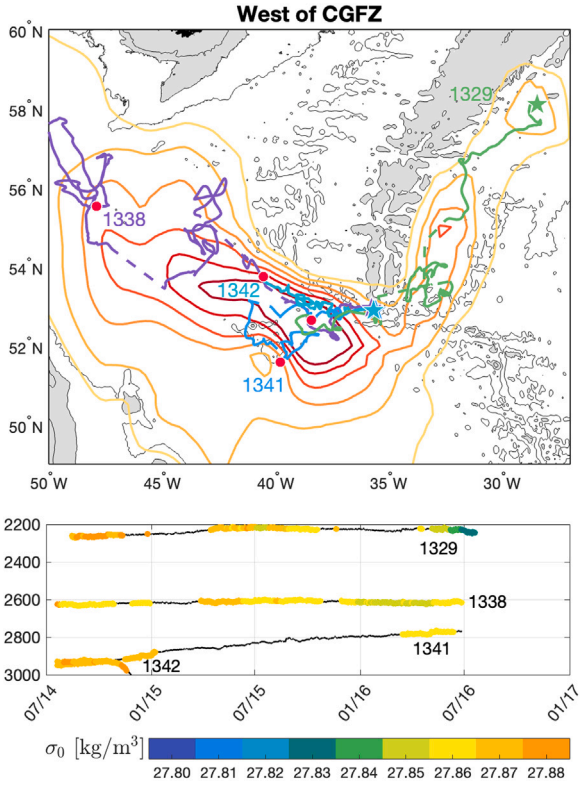

Fig. 12. Same as Fig. 9 except particle distribution maps are for layer 28 and RAFOS float trajectories occupy a density range of, approximately, between 27.86–27.88 kg m^{-3}.

timescales comparable to those observed in our export record, with minima in 2000–01, 2005–06, and 2012–13 and maxima in 2002–04 and 2007–08, features that align closely with those in our Reykjanes Ridge export time series.

Supporting this spin-up hypothesis, we find a strong negative correlation between the number of particles exported over the Reykjanes Ridge and the SSH gradient between the Iceland and Irminger Seas (after removing the 40-year increasing SSH trend, not shown). Specifically, years with increased export coincide with a relaxed SSH gradient, marked by anomalously low SSH in the Iceland Basin and higher SSH in the Irminger Sea (Fig. 13). This gradient is preferentially driven by SSH variability within the Iceland Basin, highlighting its dominant role in modulating interbasin exchange. Additionally, and consistent with intensified gyre dynamics, SSH contours indicate that the subpolar gyre is expanded eastward during high export years, further suggesting enhanced westward export is favored when the gyre is more strongly developed.

Although spin-ups of the subpolar gyre are often associated with positive phases of the North Atlantic Oscillation (NAO), which induces a basin-wide decrease in SSH relative to the subtropical gyre, Foukal and Lozier (2017) found that NAO variability was not directly linked to changes in the strength of the subpolar gyre. Instead, they associate gyre expansion and contraction to the East Atlantic pattern, an atmospheric mode that captures meridional shifts in the centers of wind stress curl over the North Atlantic, typically between the Irminger Sea and the Azores. This suggests that the spin-up and expansion of the subpolar gyre, and its impact on intermediate-depth transport into the Iceland Basin, may be more strongly governed by changes in wind stress curl geometry than by the NAO alone. This could explain the strong correlation observed here between Reykjanes Ridge export and the SSH gradient between the Iceland and Irminger Sea however, more work is needed to illustrate this potential linkage and to fully resolve the mechanisms controlling ISOW export across the Reykjanes Ridge.

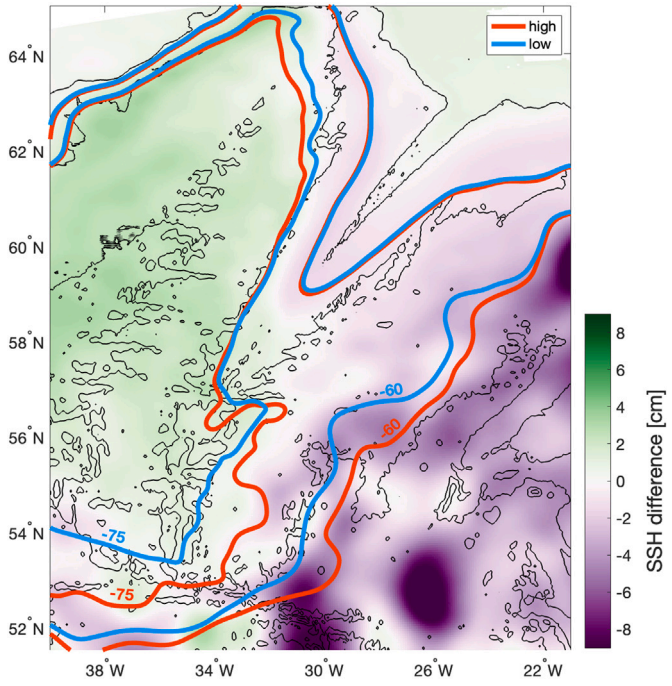

Fig. 13. Sea surface height difference between composites of high and low Reykjanes Ridge export time periods. High (low) export years are defined as years where particle export is in the top (bottom) 25% of all years. The −75 cm and −60 cm sea surface height contours are plotted for both high (red) and low (blue) export composites. The 40-year increasing SSH trend is removed at each model grid cell. Bathymetry is contoured every 1000 m.

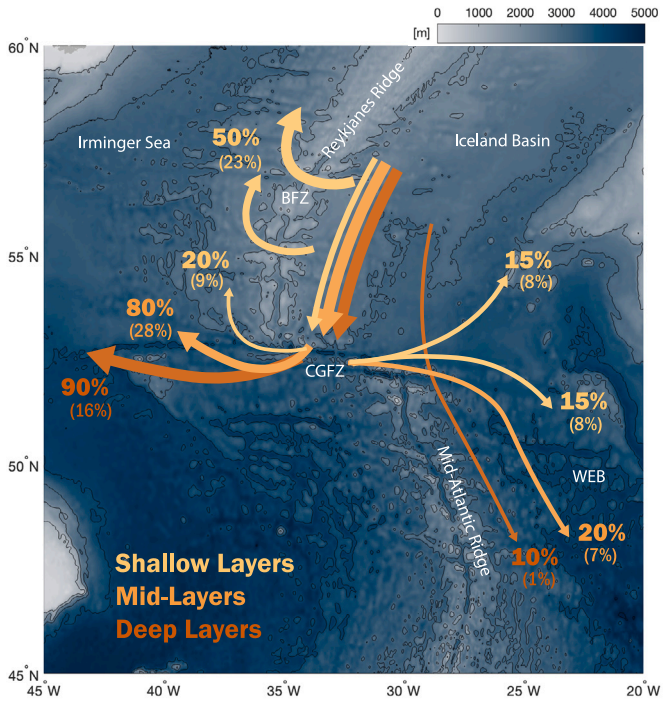

Fig. 14. Updated schematic of ISOW pathways from the Iceland Basin reflecting the depth dependency identified in this study. Light colors represent shallow layers of ISOW while dark layers represent deeper layers. Numbers in bold represent the approximate percentage of particles within the given layer to be exported along the associated pathway. Numbers in parentheses represent the approximate percentage of total particles to be exported along the associated pathway.

Export through the CGFZ is characterized by higher frequency fluctuations than that of the Reykjanes Ridge, dominated by variability between 2.5–5 years (Fig. 5B). We show that CGFZ export is closely linked to zonal surface velocities, a proxy that captures the meridional displacement of the northern branch of the NAC within the fracture zone. Specifically, a low (high) surface U velocity indicates a more southward (northward) oriented NAC which allows for more (less) ISOW export through the CGFZ. A number of studies have connected variability in NAC pathways to changes in wind stress curl over the subpolar gyre and to broader modes of atmospheric variability such as the NAO (Bower and von Appen, 2008; Roessler et al., 2015). Here, however, we were not able to reconcile CGFZ export with the NAO index and further investigation is needed to disentangle the role of atmospheric forcing in modulating the NAC and ISOW export.

Roessler et al. (2015) identifies a significant long-term trend between 1992 and 2013 marked by a more focused NAC core in the central branch and decreasing transports in the northern and southern branches. In agreement with Roessler et al. (2015), we observe a declining trend in surface U velocity beginning around 2008, however a corresponding increase in particle export through the CGFZ is not observed. Particle export does appear to increase from about 2008 to 2018 but sharply declines in the subsequent years, even as surface U velocity continues to decrease. This could be due, in part, to the lifespan of the particles as they reach the end of the model run but could also be attributed to a relatively strong Reykjanes Ridge export during the same time period which would decrease the number of particles available to reach the CGFZ. This suggests that changes in surface flow alone may not fully determine the variability in deep water export through the fracture zone.

Controls on export into the WEB are not explicitly investigated in this study. It is clear that export into the WEB increases when export through the CGFZ decreases, suggesting particles that are blocked by the NAC end up preferentially traveling southeastward into the WEB. Additionally, there is a tendency for deeper particles to follow a more direct pathway into the WEB, likely due to stronger topographic control and their reduced interaction with upper-layer circulation features such as the NAC. Particles released farther offshore from the Reykjanes Ridge also exhibit a slight preference for entering the WEB, in contrast to those released closer to the ridge, which are somewhat more likely to be exported westward over the Reykjanes Ridge.

Fig. 14 summarizes the depth-dependent export pathways of ISOW as identified from both the particle release experiment and RAFOS trajectories deployed during the OSNAP field campaigns. In the shallowest layers, approximately 50% of ISOW is exported westward over the Reykjanes Ridge, while about 20% passes through the CGFZ. The remaining portion is either recirculated within the Irminger Sea or exported southeastward into the WEB. Denser ISOW is topographically blocked from traveling over the Reykjanes Ridge, allowing more ISOW to flow through the CGFZ. These deeper waters are less influenced by the NAC, even when displaced northward, resulting in a much higher export percentage through the CGFZ. Mid-depth particles that are deflected eastward from the CGFZ almost invariably end up in the WEB, while the deepest particles follow the most direct route into the WEB, possibly even bypassing the CGFZ entirely.

One of the major takeaways from the RAFOS float program during the OSNAP campaign was a challenge to the long-held notion that ISOW primarily exits the Iceland Basin as a cyclonic boundary current through the CGFZ and along the western flank of the Reykjanes Ridge (Zou et al., 2020; Lozier et al., 2022). This ‘traditional’ pathway, once considered dominant, now appears to be more of an exception rather than a rule. By combining simulated particles with RAFOS float trajectories organized by isopycnal layer, this study adds further nuance to that conclusion. We find that only a small fraction of ISOW, approximately 20% within the shallowest layers and less than 10% of the total,

is exported along this route. It is also possible that the time period of RAFOS deployments coincided with enhanced westward export over the Reykjanes Ridge and/or increased NAC interference in the CGFZ, both of which would bias the observed pathways. In this context, the fact that not a single float conclusively followed the traditional path becomes more understandable. Rather than labeling this pathway as an anomaly, we propose it be viewed as a less dominant and more variable export route, one that is strongly modulated by interactions with the upper ocean, particularly the dynamics of the NAC, and likely restricted to shallower, less dense layers of ISOW exiting through the CGFZ.

CRediT authorship contribution statement

Ali Johnson Exley: Writing – review & editing, Writing – original draft, Visualization, Methodology, Investigation, Formal analysis, Data curation. **Amy Bower:** Writing – review & editing, Supervision, Resources, Project administration, Investigation, Funding acquisition, Conceptualization. **Xiaobiao Xu:** Writing – review & editing, Investigation, Formal analysis, Data curation, Conceptualization. **Sijia Zou:** Writing – review & editing, Investigation, Formal analysis, Conceptualization. **Anna Pinckney:** Writing – review & editing, Visualization, Investigation, Formal analysis. **Heather Furey:** Writing – review & editing, Funding acquisition, Formal analysis.

Declaration of competing interest

The authors declare the following financial interests/personal relationships which may be considered as potential competing interests: Ali Johnson Exley, Amy Bower, Heather Furey, Anna Pinckey, Xiaobiao Xu reports financial support was provided by National Science Foundation. Sijia Zou reports financial support was provided by National Natural Science Foundation of China. If there are other authors, they declare that they have no known competing financial interests or personal relationships that could have appeared to influence the work reported in this paper.

Acknowledgments

The authors gratefully acknowledge the support from the Physical Oceanography Program of the U.S. National Science Foundation Grants OCE-1948505, OCE-1756361 and OCE-1259618. S.Z. also acknowledges support from National Natural Science Foundation of China Grant 42376005.

Data availability

HYCOM data is publicly available and can be accessed from the HYCOM data server (https://www.hycom.org/). The North Atlantic HYCOM simulation can be accessed by request to X.X. RAFOS float data can be accessed at Woods Hole Ocean Access Server (https://doi.org/10.26025/1912/24388). Citation: Furey, H., & Ramsey, A. (2019). Overturning in the Subpolar North Atlantic Program (OSNAP) RAFOS Float Data collected between June 2014 to January 2019 [Data set]. Dataset published 2019 via Woods Hole Open Access Server. https://doi.org/10.26025/1912/24388. The World Ocean Atlas dataset can be found at the National Centers for Environmental Information (https://www.ncei.noaa.gov/archive/accession/0270533). Citation: Reagan, James R.; Boyer, Tim P.; García, Hernán E.; Locarnini, Ricardo A.; Baranova, Olga K.; Bouchard, Courtney; Cross, Scott L.; Mishonov, Alexey V.; Paver, Christopher R.; Seidov, Dan; Wang, Zhankun; Dukhovskoy, Dmitry (2023). World Ocean Atlas 2023 (NCEI Accession 0270533).

References

Beaird, N., Rhines, P., Eriksen, C., 2013. Overflow waters at the Iceland–Faroe ridge observed in multiyear seaglider surveys. J. Phys. Oceanogr. 43 (11), 2334–2351.
Bleck, R., 2002. An oceanic general circulation model framed in hybrid isopycnic-cartesian coordinates. Ocean. Model. 4 (1), 55–88.
Bower, A., Furey, H., 2017. Iceland-Scotland overflow water transport variability through the Charlie-Gibbs fracture zone and the impact of the North Atlantic current. J. Geophys. Res.: Ocean. 122 (9), 6989–7012.
Bower, A.S., Le Cann, B., Rossby, T., Zenk, W., Gould, J., Speer, K., Richardson, P., Prater, M.D., Zhang, H.-M., 2002. Directly measured mid-depth circulation in the northeastern North Atlantic ocean. Nature 419 (6907), 603–607.
Bower, A.S., von Appen, W.-J., 2008. Interannual variability in the pathways of the North Atlantic current over the mid-Atlantic ridge and the impact of topography. J. Phys. Oceanogr. 38 (1), 104–120.
Chassignet, E.P., Smith, L.T., Halliwell, G.R., Bleck, R., 2003. North Atlantic simulations with the hybrid coordinate ocean model (HYCOM): Impact of the vertical coordinate choice, reference pressure, and thermobaricity. J. Phys. Oceanogr. 33 (12), 2504–2526.
Daniault, N., Mercier, H., Lherminier, P., Sarafanov, A., Falina, A., Zunino, P., Pérez, F.F., Ríos, A.F., Ferron, B., Huck, T., et al., 2016. The northern North Atlantic ocean mean circulation in the early 21st century. Prog. Oceanogr. 146, 142–158.
De Marez, C., Ruiz-Angulo, A., Le Corre, M., 2024. Structure of the bottom boundary current south of Iceland and spreading of deep waters by submesoscale processes. Geophys. Res. Lett. 51 (5), e2023GL107508.
Devana, M., Johns, W., 2024. Structure and variability of iceland Scotland overflow water transport in the Western Iceland Basin. J. Geophys. Res.: Ocean. 129 (8), e2023JC020107.
Dickson, R.R., Brown, J., 1994. The production of North Atlantic deep water: Sources, rates, and pathways. J. Geophys. Res.: Ocean. 99 (C6), 12319–12341.
Foukal, N.P., Lozier, M.S., 2017. Assessing variability in the size and strength of the North Atlantic subpolar gyre. J. Geophys. Res.: Ocean. 122 (8), 6295–6308.
Furey, H., Bower, A., Ramsey, A., Houk, A., Meunier, T., 2024. Variability of iceland Scotland overflow water across the Reykjanes ridge: 2-years of Moored observations in the bight fracture zone. J. Geophys. Res.: Ocean. 129 (6), e2023JC020463.
Hansen, B., Húsgaro Larsen, K.M., Hátún, H., Østerhus, S., 2016. A stable faroe bank channel overflow 1995–2015. Ocean. Sci. 12 (6), 1205–1220.
Hansen, B., Østerhus, S., 2000. North Atlantic–Nordic seas exchanges. Prog. Oceanogr. 45 (2), 109–208.
Hansen, B., Østerhus, S., 2007. Faroe bank channel overflow 1995–2005. Prog. Oceanogr. 75 (4), 817–856.
Hogan, T.F., Liu, M., Ridout, J.A., Peng, M.S., Whitcomb, T.R., Ruston, B.C., Reynolds, C.A., Eckermann, S.D., Moskaitis, J.R., Baker, N.L., et al., 2014. The navy global environmental model. Oceanography 27 (3), 116–125.
Johns, W.E., Devana, M., Houk, A., Zou, S., 2021. Moored observations of the Iceland-Scotland overflow plume along the eastern flank of the Reykjanes ridge. J. Geophys. Res.: Ocean. 126 (8), e2021JC017524.
Kanzow, T., Zenk, W., 2014. Structure and transport of the Iceland Scotland overflow plume along the Reykjanes ridge in the Iceland basin. Deep. Sea Res. I 86, 82–93.
Large, W.G., McWilliams, J.C., Doney, S.C., 1994. Oceanic vertical mixing: A review and a model with a nonlocal boundary layer parameterization. Rev. Geophys. 32 (4), 363–403.
Lozier, M.S., Bower, A.S., Furey, H.H., Drouin, K.L., Xu, X., Zou, S., 2022. Overflow water pathways in the North Atlantic. Prog. Oceanogr. 208, 102874.
Petit, T., Mercier, H., Thierry, V., 2019. New insight into the formation and evolution of the East Reykjanes ridge current and Irminger current. J. Geophys. Res.: Ocean. 124 (12), 9171–9189.
Petit, T., Thierry, V., Mercier, H., 2022. Deep through-flow in the bight fracture zone. Ocean. Sci. 18 (4), 1055–1071.
Racapé, V., Thierry, V., Mercier, H., Cabanes, C., 2019. ISOW spreading and mixing as revealed by deep-argo floats launched in the Charlie-Gibbs fracture zone. J. Geophys. Res.: Ocean. 124 (10), 6787–6808.
Ramsey, A., Furey, H., Bower, A., 2020. Overturning of the Subpolar North Atlantic Program (OSNAP): RAFOS Float Data Report, June 2014–January 2019. Woods Hole Oceanographic Institution Tech. Rep. Technical Report, WHOI-2020-06, p. 511. http://dx.doi.org/10.1575/1912/26515.
Roessler, A., Rhein, M., Kieke, D., Mertens, C., 2015. Long-term observations of North Atlantic current transport at the gateway between western and eastern Atlantic. J. Geophys. Res.: Ocean. 120 (6), 4003–4027.
Rosmond, T.E., 1992. The design and testing of the navy operational global atmospheric prediction system. Weather. Forecast. 7 (2), 262–272.
Rossby, T., Dorson, D., Fontaine, J., 1986. The RAFOS system. J. Atmos. Ocean. Technol. 3 (4), 672–679.
Saunders, P.M., 1994. The flux of overflow water through the Charlie-Gibbs fracture zone. J. Geophys. Res.: Ocean. 99 (C6), 12343–12355.
Saunders, P.M., 1996. The flux of dense cold overflow water southeast of Iceland. J. Phys. Oceanogr. 26 (1), 85–95.
Schott, F., Stramma, L., Fischer, J., 1999. Interaction of the North Atlantic current with the deep Charlie Gibbs fracture zone throughflow. Geophys. Res. Lett. 26 (3), 369–372.

Swift, J.H., 1984. The circulation of the Denmark strait and Iceland-Scotland overflow waters in the North Atlantic. Deep. Sea Res. A. Ocean. Res. Pap. 31 (11), 1339–1355.

Uppala, S.M., Kållberg, P., Simmons, A.J., Andrae, U., Bechtold, V.D.C., Fiorino, M., Gibson, J., Haseler, J., Hernandez, A., Kelly, G., et al., 2005. The ERA-40 re-analysis. Q. J. R. Meteorol. Soc. 131 (612), 2961–3012.

Xu, X., Bower, A., Furey, H., Chassignet, E.P., 2018. Variability of the Iceland-Scotland overflow water transport through the Charlie-Gibbs fracture zone: Results from an eddying simulation and observations. J. Geophys. Res.: Ocean. 123 (8), 5808–5823.

Xu, X., Hurlburt, H., Schmitz Jr., W., Zantopp, R., Fischer, J., Hogan, P., 2013. On the currents and transports connected with the Atlantic meridional overturning circulation in the subpolar North Atlantic. J. Geophys. Res.: Ocean. 118 (1), 502–516.

Xu, X., Rhines, P.B., Chassignet, E.P., Schmitz Jr., W.J., 2015. Spreading of Denmark strait overflow water in the western subpolar North Atlantic: Insights from eddy-resolving simulations with a passive tracer. J. Phys. Oceanogr. 45 (12), 2913–2932.

Xu, X., Schmitz, Jr., W., Hurlburt, H., Hogan, P.J., Chassignet, E.P., 2010. Transport of nordic seas overflow water into and within the Irminger sea: An eddy-resolving simulation and observations. J. Geophys. Res.: Ocean. 115 (C12).

Yashayaev, I., Dickson, B., 2008. Transformation and fate of overflows in the northern North Atlantic. In: Arctic–Subarctic Ocean Fluxes: Defining the Role of the Northern Seas in Climate. Springer, pp. 505–526.

Zou, S., Bower, A., Furey, H., Susan Lozier, M., Xu, X., 2020. Redrawing the Iceland-Scotland overflow water pathways in the North Atlantic. Nat. Commun. 11 (1), 1890.

Zou, S., Lozier, S., Zenk, W., Bower, A., Johns, W., 2017. Observed and modeled pathways of the Iceland Scotland overflow water in the eastern North Atlantic. Prog. Oceanogr. 159, 211–222.